Plasmonic Nanopore with Nanopattern and Nanoparticles for Single Molecule Analysis

Seong Soo Choi, Myoung Jin Park, Sae-Joong Oh, Chul Hee Han, Yong-Sang Kim, and Nam Kyou Park*

In this report, the nano-hole on the electron beam induced membrane surrounded by periodic groove patterns are fabricated by focused ion beam technique (FIB), field emission scanning electron microscopy (FESEM), and transmission electron microscopy (TEM). Initially, a ≈200 nm thick Au films was deposited on the microfabricated pyramid, or on the flat plate by using a sputter-deposition technique. Nano-pore formation inside the FIB drilled Au aperture was controlled down to a few nanometer by using electron beam irradiations. Periodic patterns would enhance the optical intensity through the nano-aperture. Au particles were formed on the membrane several months after electron beam irradiations. In addition, surface plasmon-enhanced Raman spectroscopy measurements were performed and the greatest optical intensity from on the pyramidal aperture surrounded with the nanopattern was measured. Fabricated plasmonic pore-device can be utilized as a next generation optical sensor for single molecule analysis. TEM images of the fabricated nanopore surrounded by periodic patterns on the plate are presented with electron beam profile on the detector.

1. Introduction

We previously fabricated the nano-hole surrounded with periodic patterns. The optical transmission through the metallic nanometer size single aperture is proportional to $(d/\lambda)^4$, where d is the diameter and λ is the input wavelength. The transmitted optical intensity through the nano-aperture would be very weak, therefore, the nano-aperture surrounded by periodic patterns was designed, and the enhanced optical intensity is reported.[1–3] The solid state nanopore device for single molecule analysis is currently fabricated on a thin SiN membrane or a graphene by using high energy TEM electron beam irradiations. However, all of DNA translocation experiments are reported to have high error rates with electrical characterizations.[4,5] It may be due to electric dipole layer formation inside the pore channel. Current genome detection techniques are performed under the optical detection technique. Recently, nanoplasmonic sensing for surface plasmon resonance based on ordered flow-through nanohole array with its diameters ranging from 300 to 100 nm was reported.[6,7]

However, the nanopore with ≈10 nm diameter for an optical detection technique has yet to be fabricated. We previously reported fabrication of the nano-aperture surrounded by the periodic patterns on pyramidal probes to improve the low transmittance of light through the nano-size aperture.[8–10] We also have fabricated the nanopore with its diameter ranging from 10 to 3 nm inside the FIB drilled aperture by using various surface treatments including electron beam irradiations and ion beam irradiation.

Formation of the Au nanoparticle on the diffused membrane during the electron beam processing was also reported.[11–13] Plasmonic Au nanoparticle can provide the huge optical enhancement of 10^6-fold increase, so that it can be utilized as surface enhanced Raman spectroscopy (SERS) sensor.[14] We carried out the optical measurements by using SERS technique and observed the highest optical intensity from the aperture surrounded with the periodic nano-pattern on pyramid. The nanopore with periodic groove nano-patterns, along with the Au particles formed on the pore-containing membrane can be utilized as a plasmonic optical device for single molecule bio sensor.

Prof. S. S. Choi, Prof. S.-J. Oh, Prof. C. H. Han
SunMoon University, Sunmoon-ro, Tangjung myun, 31460, South Korea
E-mail: sscphy2010@gmail.com; sscphy1982@daum.net

Prof. M. J. Park
Korea Military Academy, Nowon-ku, Harang-ro Mailbox 77-1, Seoul, South Korea

Prof. Y.-S. Kim
Sungkyunkwan University, Jang-An-ku, Seobu-ro, Suwon 16419, South Korea

Prof. N. K. Park
Seoul National University, Shinrim-dong, Kwanak-Gu, Seoul 08826, South Korea

DOI: 10.1002/pssa.201700484

2. Experimental Section

2.1. Fabrication Procedure of the Specimen

Au nano-holes with periodic groove patterns on the pyramid, and on the flat plate were also fabricated as presented in **Figure 1**. The nano-holes on top of the pyramidal structures were fabricated using conventional Si microfabrication process such as photolithography, wet etching, stress-induced thermal oxidation, and metal sputter deposition. The detailed fabrication process is

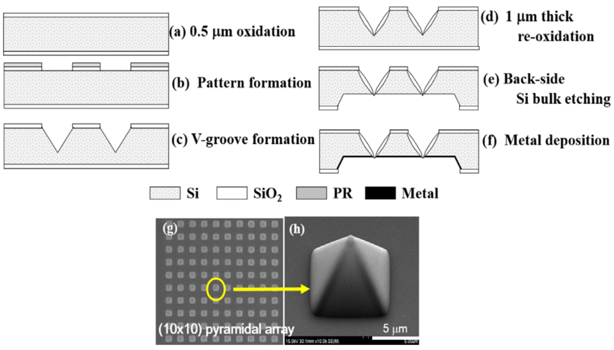

Figure 1. Fabrication process for the microfabricated pyramidal probe array in (a)–(f). FESEM images of the microfabricated (10 × 10) pyramid array (g) with a single pyramid (h).

also given elsewhere.[15,16] The stress-induced thermal oxidation provides the thinner oxide at the apex of the pyramid. After revealing the oxide pyramidal array by using a tetramethylammonium hydroxide (TMAH) etchant solution, the Au thin film was sputter deposited, followed by drilling nanoholes by using focused ion beam (FIB). The pyramidal array by tuning depth, pitch, and width of the V-groove well can be an excellent SERS substrate due to surface plasmonic effect.[17]

The flat Au plate samples were either fabricated by using plateau pyramid structures, or purchased from commercial company (www.temwindows.com).

2.2. Sample Preparation and Its Characterization

Sample preparation processes were carried out at National Nanofabrication Center (NNFC, Daejeon, South Korea), and Korea Advanced Nano Fab Center (KANC, Suwon, South Korea). Surface modifications with electron beam irradiations by using FESEM and with 30 keV focused Ga ion beam with 1.4 nA were performed with Dual Beam Helios FIB (FEI). High energy electron beam irradiations were carried out by using TEM (JEM-2010, JEM-3011 HR). Electron beam currents during specimen processing were obtained from electronic control panel display since Faraday cup was not installed for our TEM instruments. However, a big aperture on the specimen with ≈10 μm diameter were drilled to measure the electron beam currents on the fluorescent disk equipped with TEM instruments. In order to find the influence of the periodic nanopatterns on the optical intensity, 2 dimensional simulations were carried by using a commercial tool (Opti-FDTD, OptiWave).

2.3. Finite Difference Time Domain (FDTD) Simulation Analysis on the Plate and the Pyramid

Figure 2 shows the finite-difference time-domain (FDTD) simulation results for the four different situations; i) a nano-aperture on the Au plate with a 300 nm diameter with and without periodic nanopatterns in (a) and (c); ii) a nano-aperture on top of the Au pyramid with and without periodic patterns in (b) and (d).

Thickness of Au film is set to be 300 nm for both the flat plate and the pyramid. The optical intensities and the electric field through the nano-apertures are presented in the upper column and in the down column, respectively, in Figure 2.

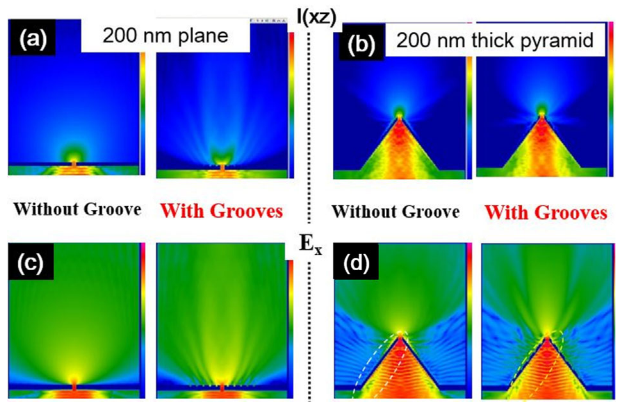

Figure 2. Optical intensities (I_{xz}) and electric fields (E_x) through Au nano-apertures are shown by using FDTD simulations on the plate and on the pyramid, with and without periodic groove patterns. (*X* axis: distance, *Y* axis: arbitrary scale). Optical intensities and electric fields intensities from the samples with periodic groove patterns greater with directionality than the sample without periodic grooves are clearly presented.

Figure 3 presents the peaks formed on the periodic grooves by using FDTD simulations. The width, the pitch, and the depth of the groove patterns are 100, 250, and 100 nm, respectively. The diameter of the aperture is designed to be 300 nm. Hot spot zone on the main hole at the center and the enhanced optical peaks at the periodic grooves are shown in Figure 3.

2.4. Fabrication of Nano-Holes Surrounded with Periodic Groove Patterns

Periodic groove patterns on the pyramids and on the flat plates were engraved by using 30 keV FIB technique (Dual Beam Helios, FEI). FESEM images were also obtained by utilizing the instrument equipped with Dual Beam Helios FIB as in **Figure 4**.

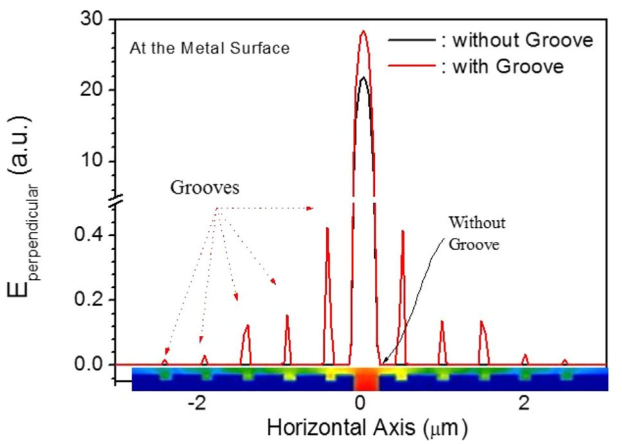

Figure 3. The peaks of the electric fields for the periodic groove patterns on the plate are shown by FDTD simulation. The diameter of the aperture is 300 nm and the width, the pitch, the depth are 100, 250, and 100 nm, respectively.

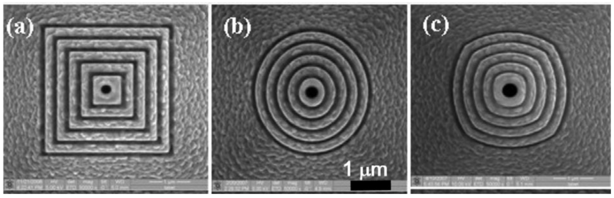

Figure 4. FESEM images of three different types of the patterns drilled on the Au deposited pyramidal structures. Square pattern, circular pattern, and elliptical patterns were drilled on pyramids as in (a), (b), and (c), respectively. The depth, the pitch, and the width is designed to be ≈100, ≈250, and 100 nm, respectively.

Square patterns and circular groove patterns cannot present the equal distance along the pyramidal wall. Hence, the elliptical groove pattern was engraved to provide the equi-distance from the pyramidal apex to the grooves along the pyramidal wall. The highest optical intensity was observed among three nano-patterns, due to the optimized interference between the localized surface plasmon in the grooves and the surface wave traveling along the pyramidal wall.[8–10]

Figure 5 present TEM images of the nano-apertures surrounded with a single groove pattern, three groove patterns, and 5 groove patterns on the flat plane. The diameter of the aperture is ≈300 nm. The width, the pitch, and the depth is designed to be 100, 500, and 25 nm, respectively.

Figure 6 shows the electron beam profile at the electron beam detector. The thickness of the specimen and the groove depth can be calculated by using electron beam profiles. The electron beam counts through the nano-aperture at the center, and the counts through the grooves, and the base counts is measured to be ≈1280, ≈850, and ≈750, respectively. Considering the thickness of the film (≈200 nm),

The depth of the groove can be estimated to be ≈20 nm.

2.5. Formation of Nanopore by Using Electron Beam Irradiations

Formation of nanopores has been carried out by using electron beam irradiations with FESEM and TEM. It is reported that for a FESEM electron beam irradiation, the aperture always shrinks (pore shrinking) regardless of the ratio of film thickness to aperture diameter. However, for a high energy electron beam irradiation by using TEM, the holes would be shrunk only for the film thickness greater than the aperture diameter.[18–20]

Figure 7 presents the TEM images of the formed membranes after 2 keV, 1.4 nA FESEM electron beam irradiations for 1 min in Figure 7(a), 3 min in Figure 7(b), and 5 min in Figure 7(c). Tiny Au particles formed during FIB drilling are also shown on the periphery of the Au apertures in Figure 7(b) and (c).

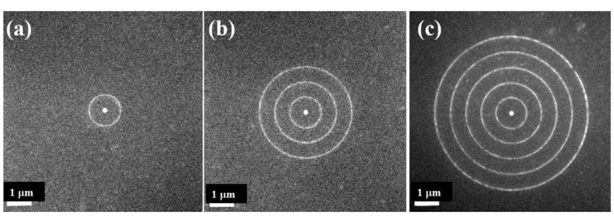

Figure 5. TEM images of the nano-aperture surrounded with a single groove pattern (a), three groove patterns (b), and 5 groove patterns (c).

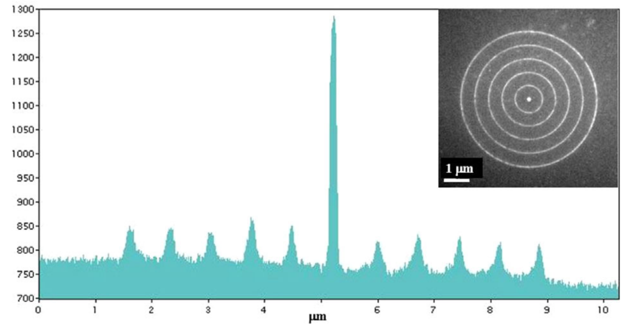

Figure 6. Electron beam profile on the detector through the groove patterns are shown. A TEM image of a nano-aperture surrounded with 5 groove pattern is inserted (top right).

Figure 8 presents the 5 nm diameter nanopore formed on the membrane on the pyramidal apex. Initially, an Au aperture with ≈86.2 nm diameter is shown after 200 nm thick Au film deposition on the SiO_2 pyramid. Numerous Au particles were shown at the periphery of the Au aperture. This can be attributed to physical characteristics of the vacuum deposited Au thin film. Vacuum deposited Au film is reported to consist of Au particles

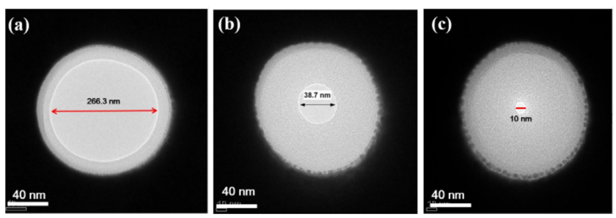

Figure 7. TEM images of pores formed under 1 min (a), 3 min (b), 5 min (c) electron beam irradiations of 2 keV, 1.4 nA. The corresponding diameters of the formed pore are measured to be 266.3, 38.7, and 10 nm, respectively.

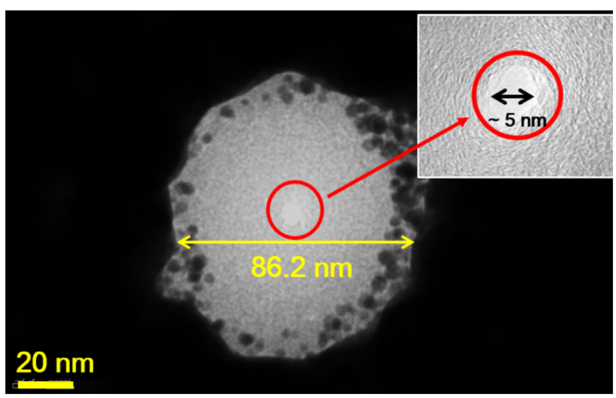

Figure 8. A TEM image of a 5 nm diameter pore at the pyramidal apex is shown. Au particles at the periphery of the aperture are also presented. Numerous Au particles are shown on the periphery of the 86.2 diameter Au aperture.

and clusters with various size and shapes such as multiple twin particles (MTP) with a decahedron shape and an icosahedron shape.[21–23] The pore with a ≈5 nm diameter was formed on the diffused membrane under 300 keV, 51pA electron beam irradiations.

Figure 9 presents controllable pore formation dependent upon the electron beam irradiation time at 300 keV. The Au aperture diameter after FIB milling was 76.59 nm. Then, 0.5 pA electron beam currents were irradiated successively for 45 min. TEM imaging were carried out with a 10 min interval. After 45 min irradiations, the pore diameter formed is measured to be 5.61 nm. The reduction rate is found to be 1.57 nm min^{-1}.

Figure 10 presents the Au particles formed on the membrane formed under 2 keV 1.4 nA electron beam irradiations. Before irradiations, the diameter of FIB drilled aperture is 521 nm. Under an electron beam irradiation, a 207 nm diameter pore was formed. In addition, the Au nanoparticles on the membrane inside the red circles in Figure 10(a) are also shown after 5 months storage under room environments. The width of the Au nanoparticle is measured to be approximately 5.61 nm, and the lattice spacing for 10 rows is measured to be 1.18 nm. Due to unstable characteristics of Au particles formed on the diffused membrane under an electron beam irradiation, it is not possible to measure exact lattice spacing.

We also drilled several holes on the diffused Au-C binary membrane by using a focused electron beam with 200 keV TEM. The diameter and the beam currents of the focused electron beam probe is ≈2 nm and ≈511 pA as in **Figure 11**).

2.6. Measurements of SERS Optical Intensities from Various Specimen Surfaces

We have carried out SERS optical intensities measurement on three different sample surfaces: i) the flat plane sample surface as control sample (black bottom line); ii) the pyramidal probe without groove patterns (red line in the middle); and iii) the pyramidal probe with elliptical periodic patterns (blue line on the top).

The greatest SERS intensity from the elliptically patterned pyramid is obtained among three samples as in **Figure 12**.

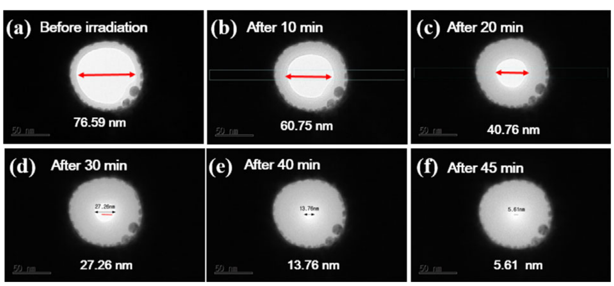

Figure 9. Controlled pore formation dependent on the electron beam exposure time at 300 keV and 0.5 pA. The FIB drilled Au aperture with 76.59 nm diameter was reduced to the pore with 5.61 nm on the formed Au-C mixture binary membrane under 45 min electron beam irradiation with 0.5 pA beam currents at 300 keV.

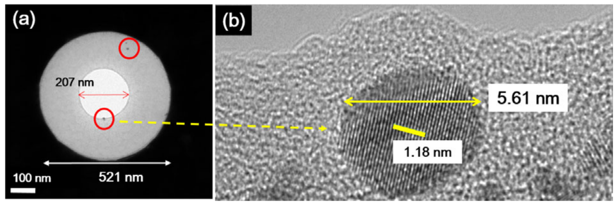

Figure 10. Two Au nanoparticles are shown on the formed membrane under 2 keV FESEM electron beam irradiations with 1.4 nA. The size of Au particle (left) on the inner side of the formed pore membrane is measured to be 5.61 nm, and the lattice spacing for 10 rows of this Au particle is found to be 1.1 nm (right).

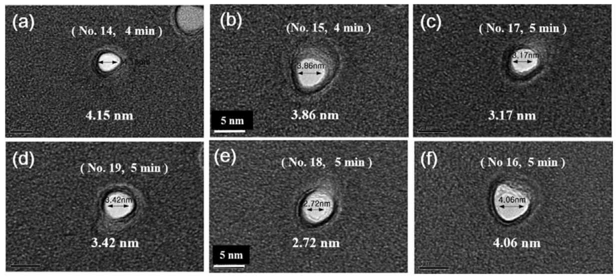

Figure 11. TEM images of the drilled pore on the Au-C binary membrane by using 200 keV focused electron beam irradiations with its 1.5 nm probe diameter and 51 pA. On this particular Au-C binary membrane, pore diameters ranging from 2.72 nm to 4.15 nm are observed after 4 ∼ 5 min electron beam irradiations. Pore drilling on the nanometer spot is found to be more dependent on the electron beam stability than the membrane chanracteristics.

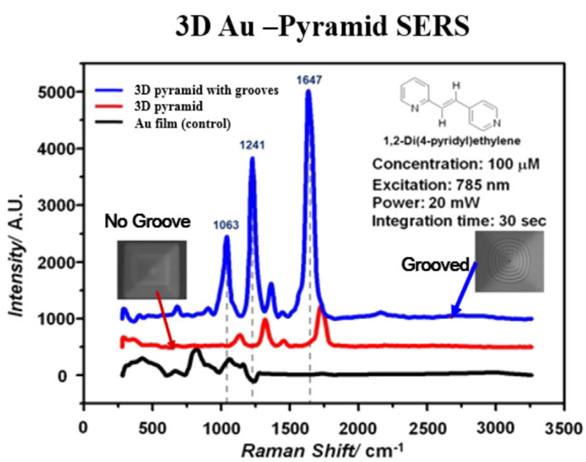

Figure 12. Surface enhanced Raman spectroscopy (SERS) optical intensity measurements for the pyramid with groove patterns (blue), the pyramid without groove patterns (red), and the flat surface without patterns (black) are shown. The highest SERS intensity from the patterned pyramidal probe is observed.

3. Summary of the Results

We have fabricated the Au apertures surrounded with periodic groove patterns on the flat plane, and on the pyramid by using a FIB technique. Then, electron beam irradiations either by FESEM or TEM were performed to obtain the pore inside the FIB drilled Au apertures. During the fabrication process, we observed the Au particles on the periphery of Au apertures formed due to thermal spike from 30 keV Ga ion beam FIB drilling, and also observed the numerous Au particles diffused under 2 keV FESEM electron beam irradiation at the pyramidal apex. Au particles on the diffused Au-C binary membrane under a room environments storage after electron beam irradiations are observed.

The fabricated pores surrounded with periodic groove patterns along with Au particles on the diffused Au-C binary membrane would provide the enhanced optical intensity, and can be utilized as next generation nanobio sensor device.

Acknowledgements

This work was supported by the research funding program (Nano-patterned Optical Nanopore for Single molecule analysis and Manipulation, 2015R1D1A1A09056781056781) under the Basic Science Research Program through the National Research Foundation (NRF) funded by the Ministry of Education, Science and Technology and the Global Research Laboratory funding (GRL; Nanoplasmonic Integrated Circuits for Ultrafast Information Processing, KRF Grant No. K20815000003, 2008-00580). The authors are also thankful for SERS optical measurements to Professor Luke Lee's group at University of California at Berkeley, CA, USA.

Conflict of Interest

The authors declare no conflict of interest.

Keywords

Au particle, electron beam induced membrane, nanopore, periodic patterns, plasmonic

Received: July 13, 2017
Revised: October 12, 2017
Published online: November 7, 2017

[1] T. W. Ebbesen, H. J. Lezec, H. F. Ghaemi, T. Thio, P. A. Wolf, *Nature* **1998**, *391*, 667.
[2] T. Thio, K. M. Pellerin, R. A. Linke, H. J. Lezec, T. W. Ebbesen, *Opt. Lett.* **2001**, *26*, 1972.
[3] H. J. Lezec, A. Degiron, E. Devaux, R. A. Linke, L. Mar-tin-Moreno, F. J. Garcia-Vidal, T. Ebbesen, *Science* **2002**, *297*, 820.
[4] A. Mikheyev, M. M. Y. Tin, *Mol. Ecol. Resour.* **2014**, *14*, 1097.
[5] E. C. Hayden, *Nature* **2015**, *521*, 15.
[6] F. Eftekharl, C. Escobedo, J. Ferreira, X. Duan, E. M. Girotto, A. G. Broto, R. Gordon, D. Sinton, *Anal. Chem*. **2009**, *81*, 4308.
[7] M. P. Jonsson, A. B. Dahlin, L. Feuz, S. Petronis, F. Hook, *Anal. Chem* **2010**, *82*, 2087.
[8] D. W. Kim, Y. C. Kim, O. Suwal, V. Jha, M. J. Park, S. S. Choi, *Mater. Sci. Eng. B* **2008**, *149*, 242.
[9] S. S. Choi, O. K. Suwal, V. K. Jha, D. W. Kim, M. J. Park, *Curr. Appl. Phys*. **2009**, *9*, S131.
[10] S. S. Choi, M. J. Park, C. H. Han, S. J. Oh, S. H. Han, N. K. Park, Y. S. Kim, H. Choo, *J. Vac. Sci. Technol. B* **2015**, *33*, 06F203-1.
[11] S. S. Choi, M. J. Park, T. Yamaguchi, S. I. Kim, K. J. Park, N. K. Park, *Appl. Surf. Sci*. **2014**, *310*, 196.
[12] S. S. Choi, M. J. Park, C. H. Han, S. J. Oh, T. Yamaguchi, N. K. Park, J. H. Yoo, K. J. Park, Y. S. Kim, *Surf. Coat. Technol*. **2016**, *306*, 113.
[13] S. S. Choi, M. J. Park, T. Yamaguchi, C. H. Han, S. J. Oh, S. I. Kim, J. H. Yoo, K. J. Park, Y. S. Kim, N. K. Park, *Sens. Bio-Sens. Res*. **2016**, *7*, 153.
[14] F. J. García-Vidal, J. B. Pendry, *Phys. Rev. Lett*. **1996**, *77*, 1163.
[15] S. S. Choi, J. T. Ok, D. W. Kim, M. Y. Jung, M. J. Park, *J. Kor. Phys. Soc*. **2004**, *45*, 1659.
[16] D. W. Kim, M. J. Park, C. H. Han, S. S. Choi, *Nanotechnology* **2005**, *16*, S304.
[17] N. M. B. Perney, F. J. García de Abajo, J. J. Baumberg, A. Tang, M. C. Netti, M. D. B. Charlton, M. E. Zooro, *Phys. Rev. B* **2007**, *76*, 035426.
[18] A. J. Storm, J. H. Chen, X. S. Ling, H. W. Zanbergen, C. Dekker, *Nat. Mater.* **2003**, *2*, 537.
[19] A. S. Prabhu, K. J. Freedman, J. W. F. Robertson, Z. Nikolov, J. J. Kasianowicz, M. J. Kim, *Nanotechnology* **2011**, *22*, 425302.
[20] H. Chang, S. M. Iqbal, E. A. Stach, A. H. King, N. J. Zaluzec, R. Bashir, *Appl. Phys. Lett*. **2006**, *88*, 103109.
[21] T. Komoda, *J. Phys. Soc. Jpn*. **1968**, *7*, 27.
[22] D. W. Pashlemy, J. Stowellm, H. Jacob, T. J. Law, *Philos. Mag.* **1964**, *10*, 127.
[23] S. Ino, *J. Phys. Soc. Jpn*. **1966**, *21*, 346.